



Using heavy metals to detect the human disturbances spatial scale on Chinese Yellow Sea coasts with an integrated analysis

S.B. Fang^{a,b,*}, C. Xu^c, X.B. Jia^c, B.Z. Wang^c, S.Q. An^c

^a Environmental Science and Engineering Department, Fudan University, Shanghai 200433, China

^b College of Fisheries and Life Science, Shanghai Ocean University, Shanghai 201306, China

^c Institute of Wetland Ecology, School of Life Science, Nanjing University, Nanjing 210093, China

ARTICLE INFO

Article history:

Received 17 February 2010

Received in revised form 9 August 2010

Accepted 15 August 2010

Available online 21 August 2010

Keywords:

Characteristic scale detection

Coastal ecosystems

Heavy metals

Human impact index

Multivariate statistics

ABSTRACT

An integrated approach involving landuse patterns obtained from landuse data and heavy metal contents of the top 10 cm surface soil layer samplings was proposed to detect the characteristic spatial scale of non-point source human disturbances on the Yellow Sea coast in China. Circular plots, with radii of 200, 500, 1000, 1500, and 2000 m were set up to represent five spatial scales. We proposed a human impact index (HII) using the landuse data to model the human disturbances. Multivariate statistics of the 10 heavy metals, Cr, Co, Fe, Mn, Ni, V, Zn, Cu, Ti, and Sr, were done. Finally curve estimation between HII and heavy metals was also done. The results showed that: (1) multivariate statistics, including principal component analysis, cluster analysis and the 1-tailed Pearson correlation analysis showing that elements Cr, Cu, Fe, Mn, Ni, V, Zn, and Co could be interpreted as anthropogenic elements and (2) of all the heavy metals showing statistical significance from the curve estimation, in general, the 1000 m scale HII had the best modeling result. We concluded that the characteristic spatial scale of human disturbances on Yellow Sea coast might be 1000 m.

Crown Copyright © 2010 Published by Elsevier B.V. All rights reserved.

1. Introduction

The question of scale has long been an important question for both cartographers and ecologists [1–3]. It is critical that when we do some research on spatial patterns of geographical, ecological, or biological phenomena we must make sure the patterns are studied on the appropriate scale [4–6]. The choice of the appropriate scale has always been an important issue in spatial ecology [7–11]. Findlay and Zheng [12] defined the characteristic spatial scale for a stressor as the nearest distance from the source at which stressor values could not be statistically distinguished from those further away, while the characteristic time scale was the length of time required to detect a statistically significant decline in average stressor values within the defined characteristic spatial scale in response to reduced stressor emission at the source.

The issue of appropriate spatial and temporal scale is not just of scientific concern, but it is also relevant to ecosystem management [13,14]. Ecosystem management is increasingly viewed and implemented as a multi-stakeholder process in which different interests are brought together in an attempt to determine desirable endstates for the ecosystem [15,16]. In this context, the scale

is particularly important, for if we choose a management scale that is larger or smaller than the characteristic scale, the benefit weighting and trade-off-making process could not be realized or might be unjustified [12,17]. Furthermore, from an economic perspective, we should monitor and assess the landscape at an appropriate scale for costs saving [12].

Human disturbance is a major stressor to almost all kinds of ecosystems [18,19]. As an important ecotone in the world, the coastal zone is subjected to increasing human use [20–27]. How to manage human disturbances in coastal zones is critical for coastal systems sustainable development. Detecting the spatial and temporal scales of human disturbances might be the key answer to achieving a reasonable policy for human disturbances management. Though some research has been done in recent times, and some significant progress have been made on monitoring scale of human disturbance, how to detect the spatial and temporal scales of human disturbances in a landscape context is still an outstanding question.

Findlay and Bourdages [28] found that the negative effects of historical road densities were detected on adjacent lands up to 1 or 2 km from a wetland. They queried the current Canadian provincial and federal wetland policies as the designated buffer zones in which road construction was prohibited, extends at most several hundred meters from the wetland's edge. Houlihan [29] found that landscape modification up to 2000–4000 m from a wetland

* Corresponding author.

E-mail addresses: bsfang@shou.edu.cn, bsfang@fudan.edu.cn (S.B. Fang).

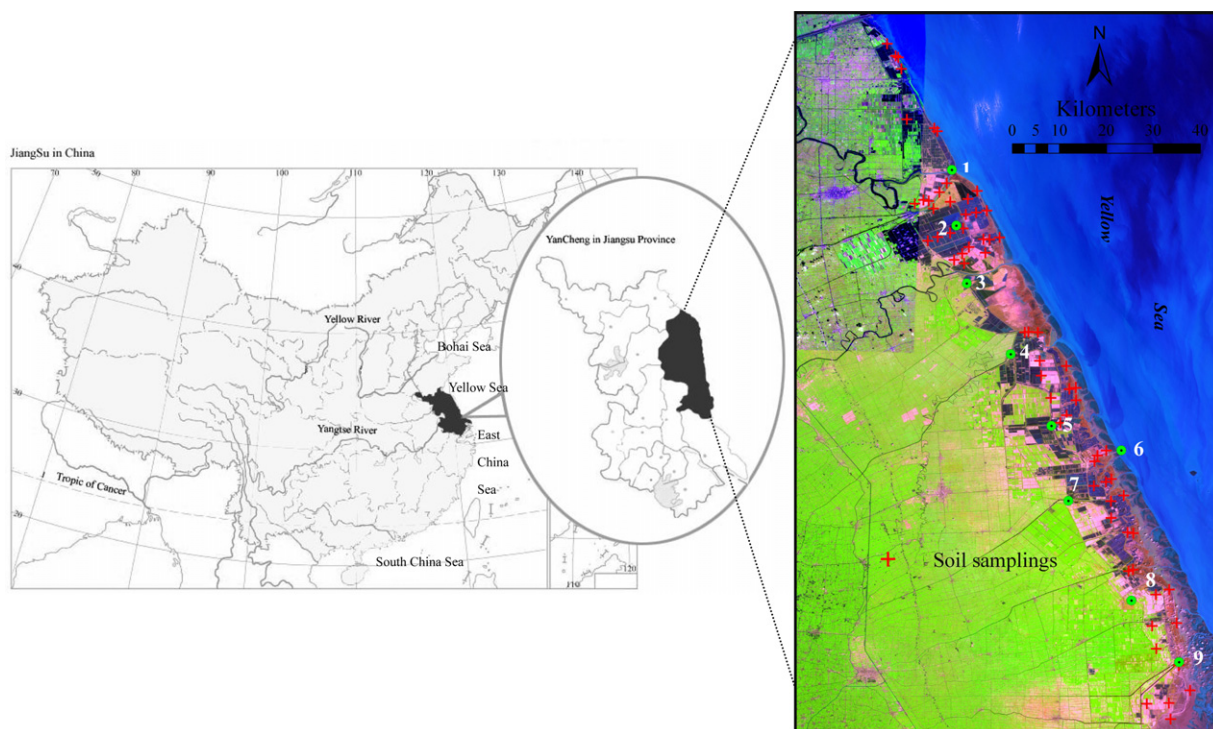


Fig. 1. the Yellow Sea coasts as the study site. Two national natural reserved lands, the Red Crown Crane National Reserved Lands, and the Dafeng Milu National Reserved Lands locate on the Yellow Sea coasts. It had been taken as a hotspot of biodiversity conservation since 1980s. Coastal area in this region has been impacted more and more because of exploded human pressures in recent time.

edge had the strongest correlations with wetland water quality and amphibian species richness, while landuse within 250–400 m from the wetland edge had the strongest correlation with plant species richness. He argued that the Ontario wetland policy which evaluated and protected wetland on a site-by-site basis and only regulated adjacent land-use out to 120 m from the wetland edge was not likely to ensure long-term protection of wetland water quality and biodiversity in Ontario.

Human disturbances in coastal China have enhanced the concentrations of heavy metals in recent years [30–38]. Heavy metals could be chosen as indicators of human disturbances. In coastal China, the main human disturbances inducing heavy metals are: urbanization [30], agriculture, aquaculture farming [31,35,36], coastal tideland reclamation [34], and industry [32,33]. Some reported human-induced heavy metals detected in coastal China include Cu, Pb and Zn in Hongkong [30], Cu, Ni, Pb, and Cd in Shanghai [38], Cu, Zn, Pb, and Hg in Jiangsu [32,35], Cu, Pb, Cd, and Zn in Jiaozhou Bay [37], Cd, Zn, and Ni in the Pearl River inlet [34].

Land use and landcover change (LUCC) analysis has been proven to be an effective way to reflect human disturbance [39–42]. Brooks et al.'s [40], and Brown and Vivas's [41] works proved that scale analysis could be done with LUCC data. Wickham et al. [43] suggested that human disturbance could be reflected with the simple selected index, and our Milu conservation work [42] also proved this index could be very powerful to indicate some spatial process.

The present study has two goals: First, we want to use a simple human impact index model, which is obtained from land use data [42], and integrate it with a soil heavy metal analysis on the Yellow Sea coast, to test if the human disturbances characteristic spatial scale defined by Findlay and Zheng [12] could be detected. Secondly, on Chinese coastal regions, the buffer zones up to a distance of 200 m from the wetlands are taken as the forbidden regions in which human disturbances are strictly controlled. Therefore, if the characteristic spatial scale can be

detected, we want to determine whether it is robust enough that only the 200 m buffer zones are managed on Chinese coastal region.

2. Study site

The study site is located at $N32^{\circ}35'–34^{\circ}28'$, and $E119^{\circ}37'–120^{\circ}53'$, along the Yellow Sea coast (Fig. 1). Lying at the north subtropical zone, the annual average precipitation is 1010 mm, and the annual average temperature is between 13.7 and 14.8 °C. The site is a plain sedimentary geomorphology formed by the river fluvial and coast sediment processes since the end of the late Pleistocene. The soils along the coast could be classified into three classes according to the formation process: Anthrosols, Fluvisols, and Cambisols [44]. Along the coast, the vegetation community is simple, distributed with a stratified pattern, from the coast to inland, lying with the bare tidal flats, *Spartina alterniflora* community, *Suaeda glauca* Bge community, *Imperata cylindrica* (Linn.) Beauv. community and *Phragmites australis* community, and lastly other xeromorphic vegetation. Human-induced landuse along this coastal region includes mainly agriculture farming, aquaculture, and solar salt production. In recent times, human activities of harbor building, wind power generation, and tourism have increased. These activities have just happened within the last 2 years, and the associated sewage and solid wastes are treated collectively so we only consider the typical non-point pollution sources including agriculture farming, aquaculture, and solar salts production in this study.

Two national natural reserved wetlands, the Red Crown Crane National Reserved Lands, and the Dafeng Milu National Natural Reserve are located on this coast. The core region is located on the Yancheng coast. It has become the hotspot of wetland research for its significance in biodiversity conservation. In 1992, Yancheng was listed in the world network of biosphere conservation (WNBP) by the United Nations.

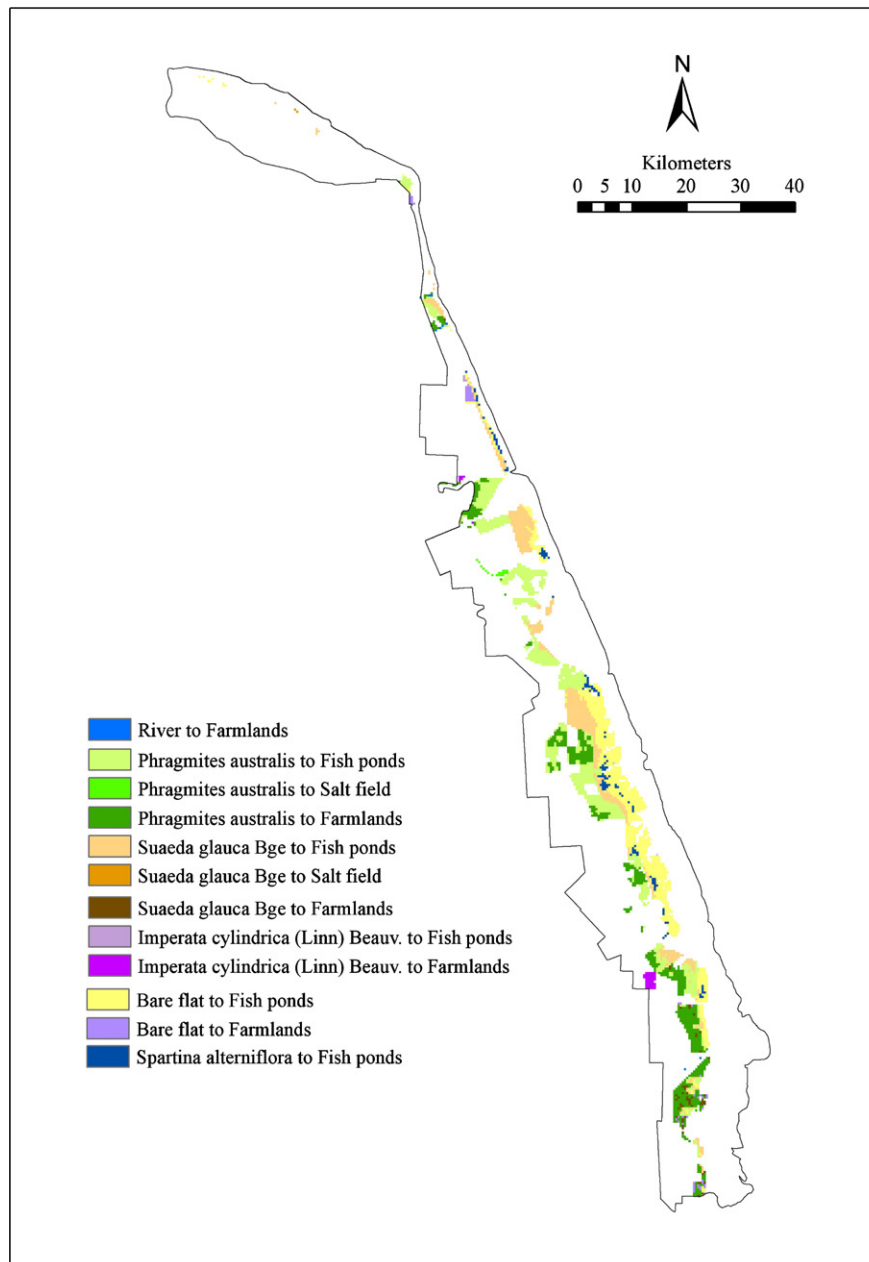


Fig. 2. The changing patterns of the coastal landuse from 1991. We gave the landscape transformed information from other landscapes to the main human-dominated landscapes, including farmlands, solar salts production, and aquaculture since 1991–2006.

Since 1991, 29.5% of land has been transformed to farmlands, aquaculture lands, and solar salt fields (Fig. 2).

3. Methods

The analysis was done by four steps: First, a simple human impact index (HII) reflecting the human disturbances along the coast was proposed using the landuse data in 2006; secondly, within the human-dominated landscape along the coast we sampled 66 top 10 cm surface soil layer samples to test for heavy metals; then, using the statistical methods of the principal component analysis (PCA), cluster analysis (CA), and correlation matrix to analyse the amount of human-induced heavy metals [33,38,45,46]; thirdly, from every soil sampling

point, five scales of circles were plotted, to model the different spatial scales. Within every circle we computed the HII. Finally, we analysed the relation between the HII of every scale and the human-induced heavy metals to determine if the characteristic spatial human disturbances scale could be detected.

The HII was computed as follows:

$$HII = P_{\text{Salt}} + P_{\text{Farm}} + P_{\text{Aqua}}$$

where P_{Salt} was the salt field area percentage in every circle plot, P_{Farm} the agriculture, and P_{Aqua} the aquaculture. This index was developed based on the work of Brooks et al. [40] and Brown and Vivas [41]. Of all the landscape metrics, the area percentage of landscape was more informative to indicate the related environmental

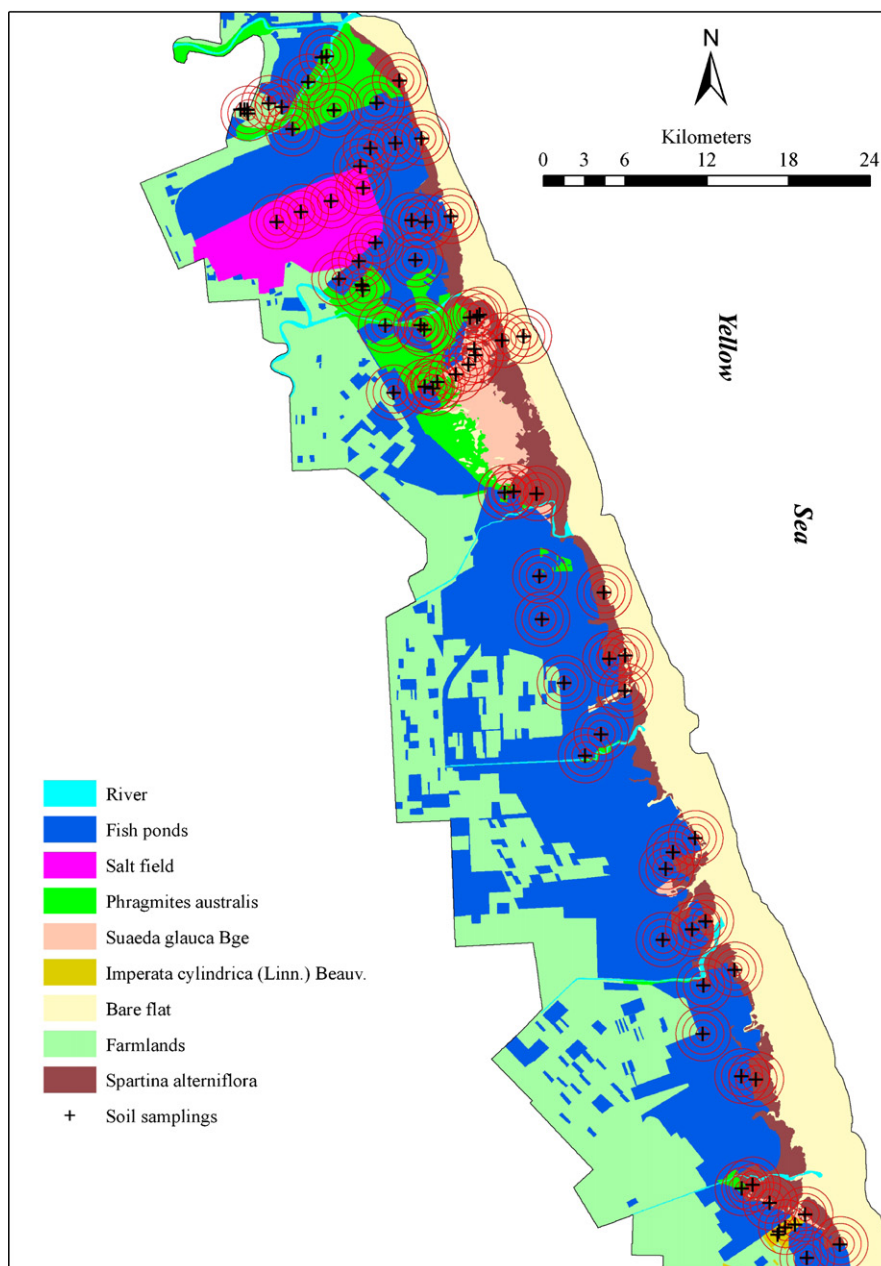


Fig. 3. Method of circles' drawing to represent different human disturbances spatial scales. From the 3rd repetition of each soil point, different radius circle plots were drawn. Circular plots, with radii of 200, 500, 1000, 1500, and 2000 m were set up to represent five spatial scales of human impact index (HII). In each circle, we computed $HII = P_{\text{Salt}} + P_{\text{Farm}} + P_{\text{Aqua}}$, where P_{Salt} is the salt field area percentage in every circle plot, P_{Farm} , the agriculture, and P_{Aqua} , the aquaculture. HII reflects the main types of human disturbances on the Yellow Sea coast.

effects [47,48]. And these three landuse types were the dominant human disturbed types in this region, so we computed HII as above.

A total of 66 soil samples were collected during September to October in 2007. Five sampling repeats, with the "W" shape, from one to another, at the distance of 50–100 m, were collected for each soil point (Fig. 1). For each repetition only the top 10 cm soil layer was sampled [38,45,46,49]. If the samples are located within an aquaculture landscape, we sampled the surface 10 cm bottom silt with a boat, but if located in a discharged pond the bottom flat was sampled.

After air-drying, all the five soil repeats were blended and then sieved with 0.15 mm screen. Metal contents of Cr, Cu, Fe, Mn, Ni, Sr, Ti, V, Zn, and Co were analysed using the inductively coupled plasma (ICP) in

the Testing and Analysis Center of Nanjing University.

From the 3rd repetition of each soil point, different radius circle plots were drawn. Five different circle plots, 200, 500, 1000, 1500, and 2000 m, were used to compute the different scales of HII (Fig. 3). This method of circle drawing to represent different human disturbances spatial scales could be referenced from the work of Brooks et al. [40], and Brown and Vivas [41].

Using SPSS software (version 15.0 for Windows), factor analysis of principal component analysis (PCA) was carried out. PCA was employed to infer the hypothetical source of heavy metals (natural or anthropogenic). The components of the PCA were rotated by a Varimax rotation. Then, rescaled the value to 0–1 ratio, with the Squared Euclidean distance method, the between-groups linkage

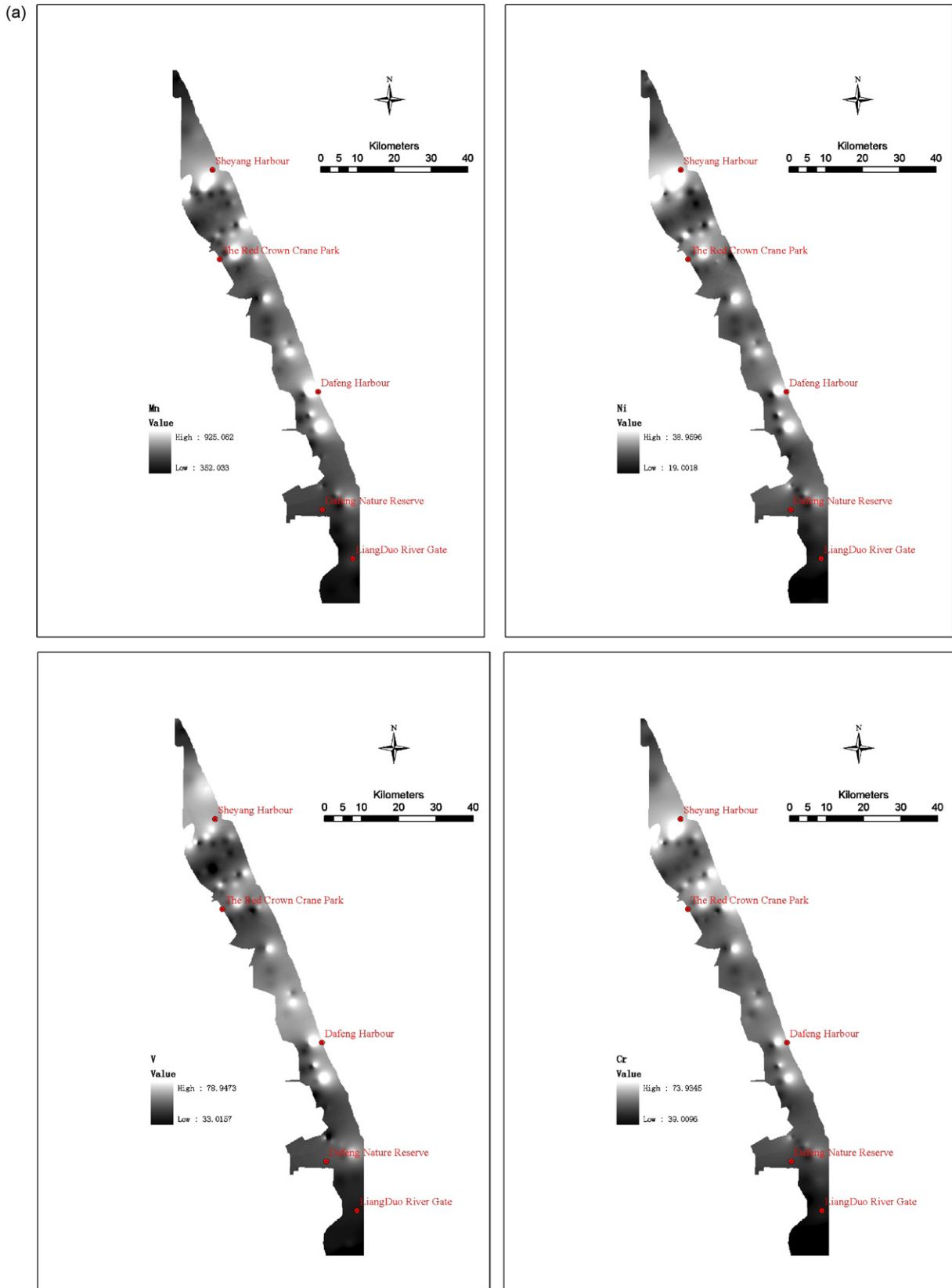


Fig. 4. Heavy metal (HM) and HII distribution patterns according to inverse distance weighted interpolation. (a) HM distribution patterns. (b) In the 1 km windows, using soil sampling points as the center, we computed the HII, then we interpolated them by ARCGIS 9.2.

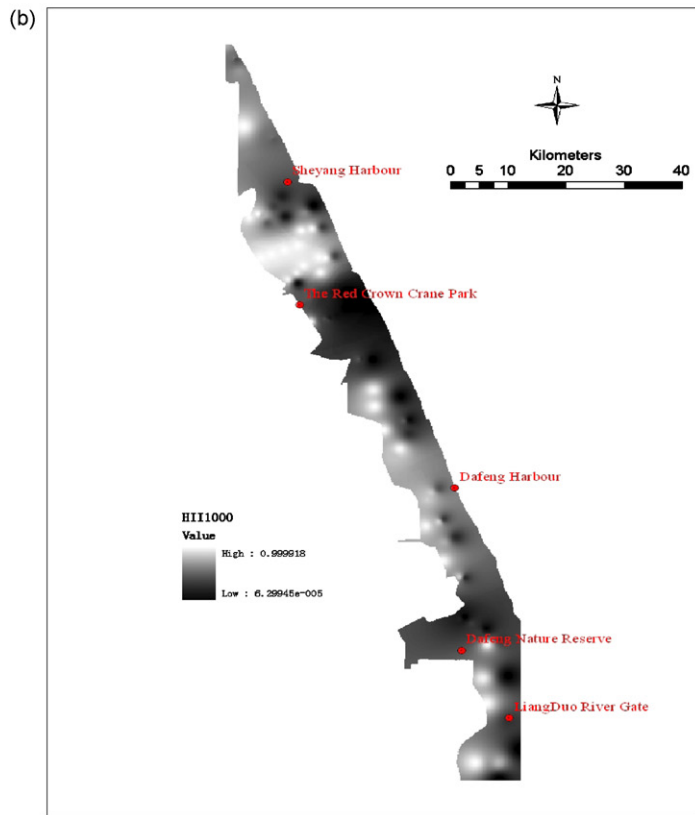
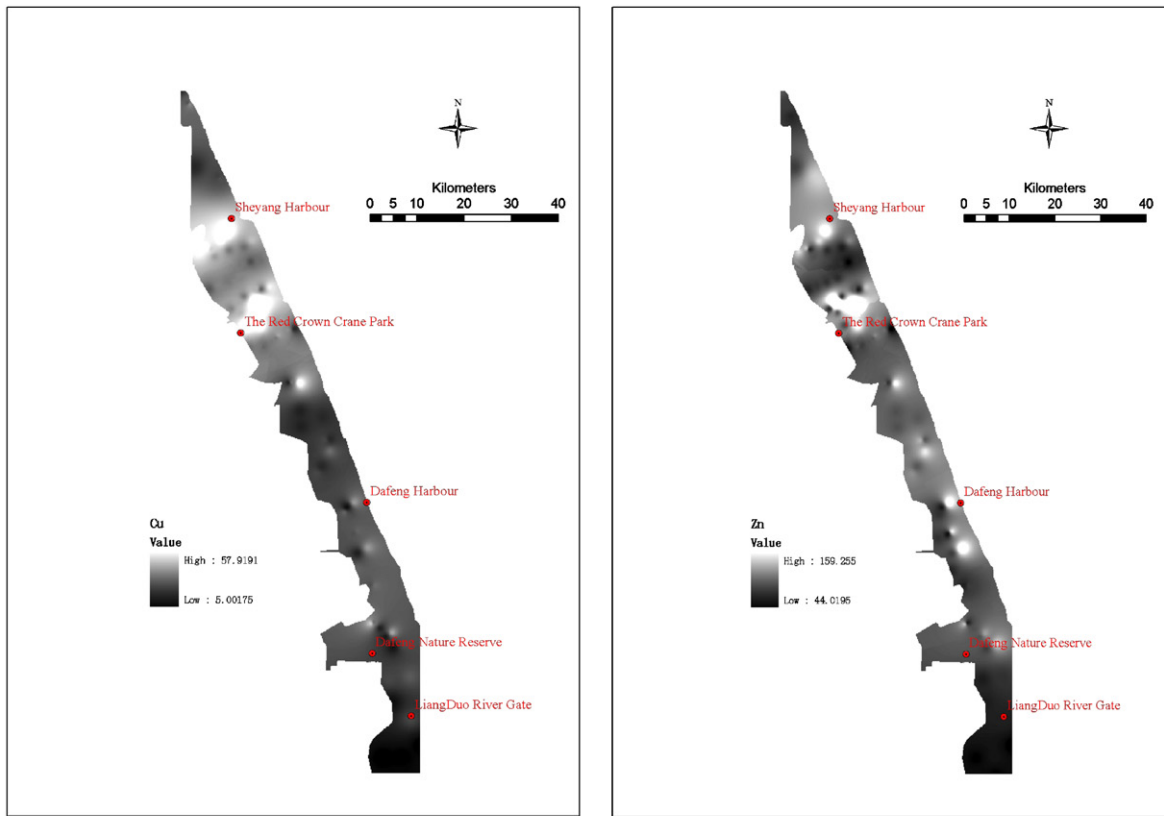


Fig. 4. (Continued).

Dendrogram using Average Linkage (Between Groups)

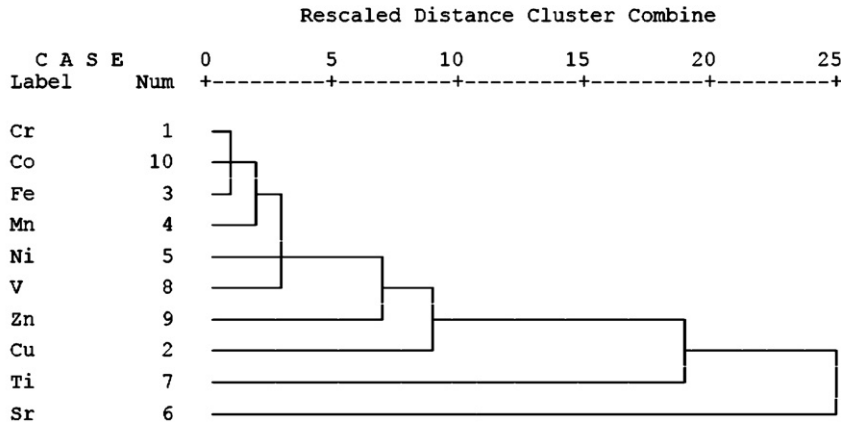


Fig. 5. Clustering analysis result revealed three clusters of elements: the first one (C1) included elements (Cr, Cu, Fe, Mn, Ni, V, Zn, and Co), which were interpreted as anthropogenic induced heavy metals.

vertical CA of the 10 metals was also carried out. Lastly, we did the 1-tailed Pearson correlation analysis of the 10 heavy metals to identify the relationship between the ten elements. From these statistical analysis methods, comparing with other reports on coastal China, and also comparing the average value with the background value of the metals, we wanted to screen the metals that were mainly human-induced along the region.

Using the HII of different scales as an independent variable, we did linear, quadratic, and cubic curve estimation with the heavy metal contents and the best estimated curve was identified. Finally, comparing the statistical significance of different scales HII with the heavy metals, we wanted to see if this method would be helpful to realize the character human disturbances spatial scale detecting defined as Findlay and Zheng [12].

4. Results

4.1. The statistical analysis of the 10 heavy metals

First we did an initial spatial pattern analysis to determine the relationship between anthropogenic disturbances and HM on a qualitative basis. Using ArcGIS software (ESRI, Redlands, CA, USA)

we obtained inverse distance weighted (IDW) interpolation of some human-induced HM referenced from other reports [30–38] and HII. IDW is a rapid, but exact, deterministic interpolator requiring minimal adjustment of model parameters and no priori data assumptions.

Our data showed that these metals have higher concentrations in regions that were characterized by substantial human development (Fig. 4). At the Sheyang Salt Field most metals were found to be present at elevated levels, while at the Liangduo River Gate only Co was present at a substantially higher concentration. In general, the Yellow Sea coasts in North Jiangsu have had a long history of human disturbance that exceeds the southern region. It is not surprising, therefore, that HM concentrations were higher in the north.

4.1.1. PCA of the 10 heavy metals

The results of PCA for heavy metal contents were presented in Table 1. Heavy metals were grouped into a three-component model, which accounted for 87.03% of all the data variation. In the rotated component matrix, the first PC (PC1, variance of 64%) included Cr, Cu, Fe, Mn, Ni, V, Zn, and Co, the second PC (PC2, variance of 13.9%) was constituted by Ti, and the third PC (PC2,

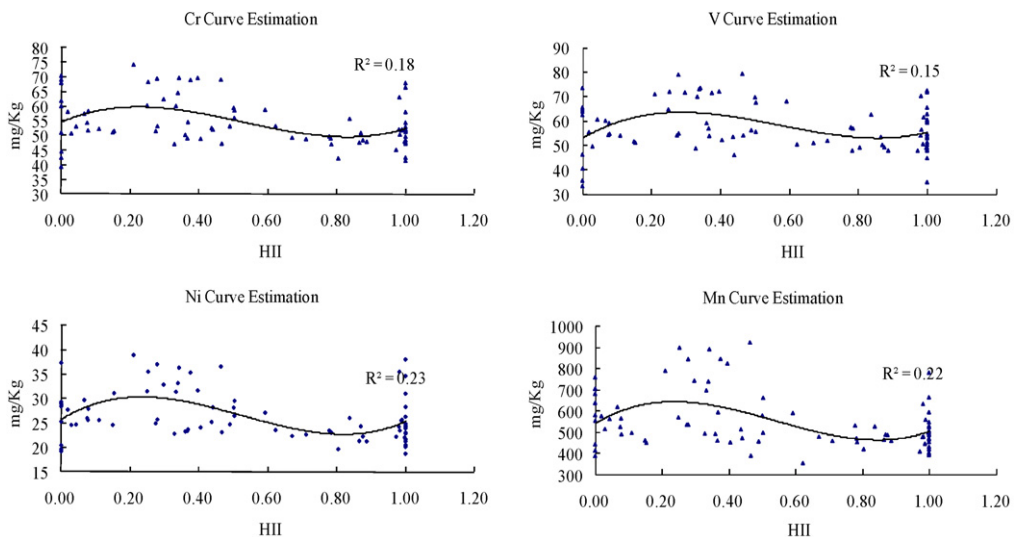


Fig. 6. Regression models showing statistical significance between metals and 1000 m radius circle HII plots. We showed the regression model between 1000 m circle plots HII with metals ($p < 0.05$).

Table 1
Total variance explained and component matrixes for total heavy metal contents (three-components extracted).

| Component | Initial eigenvalues | | | Extraction sums of squared loadings | | | Rotation sums of squared loadings | | |
|-----------|---------------------|---------------|--------------|-------------------------------------|---------------|--------------|-----------------------------------|---------------|--------------|
| | Total | % of variance | Cumulative % | Total | % of variance | Cumulative % | Total | % of variance | Cumulative % |
| 1 | 6.739 | 67.386 | 67.386 | 6.739 | 67.386 | 67.386 | 6.4 | 64.002 | 64.002 |
| 2 | 1.053 | 10.532 | 77.917 | 1.053 | 10.532 | 77.917 | 1.392 | 13.916 | 77.917 |
| 3 | 0.911 | 9.113 | 87.031 | 0.911 | 9.113 | 87.031 | 1.079 | 10.790 | 87.031 |
| 4 | 0.562 | 5.615 | 92.646 | | | | | | |
| 5 | 0.404 | 4.04 | 96.686 | | | | | | |
| 6 | 0.129 | 1.287 | 97.973 | | | | | | |
| 7 | 0.11 | 1.105 | 99.077 | | | | | | |
| 8 | 0.066 | 0.659 | 99.736 | | | | | | |
| 9 | 0.017 | 0.174 | 99.91 | | | | | | |
| 10 | 0.009 | 0.09 | 100 | | | | | | |
| Elements | Component matrix | | | Rotated component matrix | | | | | |
| | PC1 | PC2 | | PC3 | PC1 | PC2 | PC3 | | |
| Cr | 0.985 | 0.022 | | 0.031 | 0.948 | 0.263 | -0.065 | | |
| Cu | 0.731 | 0.306 | | -0.131 | 0.790 | -0.064 | 0.132 | | |
| Fe | 0.989 | 0.082 | | -0.006 | 0.971 | 0.206 | -0.030 | | |
| Mn | 0.909 | 0.102 | | 0.066 | 0.885 | 0.240 | 0.029 | | |
| Ni | 0.942 | 0.07 | | -0.206 | 0.957 | 0.027 | -0.130 | | |
| Sr | -0.178 | 0.863 | | 0.445 | -0.073 | -0.038 | 0.984 | | |
| Ti | 0.407 | -0.413 | | 0.782 | 0.170 | 0.958 | -0.033 | | |
| V | 0.887 | -0.139 | | 0.138 | 0.802 | 0.402 | -0.146 | | |
| Zn | 0.8 | -0.045 | | -0.123 | 0.783 | 0.114 | -0.178 | | |
| Co | 0.957 | -0.005 | | -0.059 | 0.931 | 0.191 | -0.128 | | |

Extraction method: principal component analysis; rotation method: Varimax.

variance of 10.8%) was constituted by Sr. PC1, including Cr, Cu, Fe, Mn, Ni, V, Zn, and Co, can be defined as an anthropogenic component, compared with other reports on other coastal regions in China [30–38]. We also compared the average with the background value of heavy metals [49]. The average value was generally higher than the background value. The background values were obtained from four sample columns with length of 100 cm at Doulong Gate [36,49]. This also could prove that these metals were human induced (Table 2).

4.1.2. CA of the 10 heavy metals

The same grouping was obtained from the clustering analysis (Fig. 5). Results revealed three clusters of elements: the first one (C1) included the elements (Cr, Cu, Fe, Mn, Ni, V, Zn, and Co) that had previously been interpreted as anthropogenic elements.

4.1.3. The 1-tailed correlation matrix of the 10 heavy metals

Results obtained from PCA were confirmed by the Pearson correlation analysis (Table 3). Anthropogenic metals were significantly correlated with each other.

4.2. The curve estimation between the HII in 2006 with the human-induced heavy metals

4.2.1. Model summary and parameter estimates with the 1000 m circle plots in 2006

From the statistical analysis and other heavy metal research cases along the Chinese coastal region [30–38], metals including Cr, Cu, Mn, Ni, V, and Zn, which were mainly human-induced, were chosen with which to do the curve estimation between the HII in 2006. The Cubic estimation model, for all other scales HII except

Table 2
Comparison between the average with the background value of heavy metals on the Yellow Sea Coast (mg/kg).

| | Cr | Mn | Ni | V | Zn |
|-----------------|-------|--------|-------|-------|-------|
| Average | 54.10 | 541.39 | 26.41 | 57.20 | 63.02 |
| Background [49] | 46.71 | 375.19 | 21.68 | 60.00 | 60.69 |

the 200 m scale, was the best to do the estimation analysis, as the 1000 m scale (Table 4). So we adopted the cubic estimation model to detect the human disturbances spatial characteristic scale.

4.2.2. The characteristic spatial human disturbances scale

4.2.2.1. Metals showing statistical significance with different scales HII in 2006. Of the five scales HII curve estimation, the 500 and 1000 scales HII showed statistical significance with metals including Cr, Mn, Ni, and V ($p < 0.05$, Table 5). The 1500 and 2000 scales HII showed statistical significance with the following metals: Cr, Mn and Ni. Only the 200 scale HII showed statistical significance with Mn and Ni.

4.2.2.2. Comparison of models between different scales HII with metals in 2006. Of all the heavy metals showing statistical significance using the cubic estimation, in general, the 1000 m scale HII showed the best statistical significance (Table 5). The metals showing statistical significance with 1000 m scale HII, including Cr, Mn, Ni, and V, had either the biggest F value, or the more significant statistical relationship. Cr had the biggest F value and the better statistical significance with the 1000 m scale HII. Mn and Ni had the biggest F value with the 1000 m scale HII, while V had the better statistical significance. We showed the curve estimation model between HII in 2006 with the above heavy metals (Fig. 6).

5. Discussion

Human disturbance is the main source of heavy metals in the top 10 cm surface soil layer in this study. Hydrological condition, location of the sewage outlet, reclamation, tidal flats location, and percentage of soil clay all can affect the heavy metal elements accumulation [34]. For three reasons we are sure that human disturbances are the main induced sources of heavy metals in this study: (1) most of our soil samples were distributed within the human-dominated landscape (Fig. 1). Lands of *P. australis* are classified as one type of landuse having significance in biodiversity conservation [42]. But within the Yellow Sea coast, *P. australis* are cultivated for papermaking, wastewater treatments through

Table 3
Correlation matrix of total heavy metal contents.

| | Cr | Cu | Fe | Mn | Ni | Sr | Ti | V | Zn | Co |
|----|---------|---------|---------|---------|---------|--------|---------|---------|---------|----|
| Cr | 1 | | | | | | | | | |
| Cu | 0.754** | 1 | | | | | | | | |
| Fe | 0.981** | 0.741** | 1 | | | | | | | |
| Mn | 0.891** | 0.565** | 0.921** | 1 | | | | | | |
| Ni | 0.936** | 0.687** | 0.938** | 0.835** | 1 | | | | | |
| Sr | -0.156 | -0.002 | -0.112 | -0.045 | -0.188 | 1 | | | | |
| Ti | 0.427** | 0.189 | 0.356** | 0.325** | 0.190 | -0.104 | 1 | | | |
| V | 0.850** | 0.430** | 0.874** | 0.834** | 0.805** | -0.177 | 0.445** | 1 | | |
| Zn | 0.726** | 0.557** | 0.763** | 0.636** | 0.740** | -0.185 | 0.262* | 0.701** | 1 | |
| Co | 0.944** | 0.685** | 0.938** | 0.878** | 0.916** | -0.203 | 0.342** | 0.820** | 0.710** | 1 |

* $p < 0.05$, 1-tailed.** $p < 0.01$, 1-tailed.

wetlands degradation, and building materials. *P. australis* could be taken as the human disturbed landscape. So nearly 58% of our soil samples were obtained in the highly human disturbed landscape, including farmlands, salt fields, aquaculture lands, and *P. australis*; (2) we only sampled the surface 10 cm soil layer. This layer of soil mainly reflects the accumulation of metals in recent times and (3) we compared our average metal elements value with the background value in this region (Table 2). We found that metals, if having a higher value than the background value, such as Ni and Mn, will have better modeled curve estimation (Table 5). The shallow sea water is the main water source for coastal agriculture farming, solar salts production, and aquaculture. So we believe that these elements are human induced in the 10 cm surface soil layer.

On the Yellow Sea coastal region, typical human actions, including agriculture, aquaculture, solar salts production, traffic roads building, industry and harbor building are all interacted with each other and the stressors are non-point. As Findlay and Zheng [12] pointed out, the definition must be adjusted when applied to the no-point source stressor. Findlay and Houlahan [50], Findlay and Bourdages [28], and Houlahan [29] all did helpful work in characteristic scale detection. But these works all took single wetland as the target. Our work in this study tries to research the non-point

source human stressors. Using the landuse data, by the simple HII index computed with the land use data, it is possible to quantitatively model the non-point source of anthropogenic disturbances [42].

Recent case studies prove that some heavy metals are mainly human-induced on coastal China [30–38]. In other regions, Emerson et al. [45] found a heavy metal pattern decreasing from landward to seaward at the Blackwater Estuary in the UK and anthropogenic disturbances had produced Pb, Zn, Cd, and Cu at the head of the estuary. Visuthismajarn et al. [51] reported that the use of pesticides, disinfectants, microorganisms, feed additives, vitamins, antibiotics, fertilizers, and immunostimulants, had caused the most serious potential ecological risk of heavy metals concentrations including Mn, Cd, and Cu in the abandoned shrimp ponds in Thailand. Caeiro et al. [52] reported that the most serious concentration of heavy metal was Cd, followed by As and Cu in the Sado Estuary in Portugal. Firat et al. [53] found high concentrations of Cr, Cd, Cu, Zn, and Fe in crabs and shrimps at the Iskenderum Bay in Turkey. Nemr et al. [46] reported high concentrations of Cd, Ni, and Pb and a moderate concentration of Zn in the sediments of the Suez Gulf. These results reveal that heavy metals could be chosen as human

Table 4
Model summary and parameter estimates between the 1000 m scales HII with total heavy metal contents.

| Equation | Model summary | | | | Parameter estimates | | | |
|------------|---------------|------|-------|-------|---------------------|---------|----------|---------|
| | R^2 | F | $df1$ | $df2$ | Constant | $b1$ | $b2$ | $b3$ |
| Cr | | | | | | | | |
| Linear* | 0.07 | 4.48 | 1.00 | 64.00 | 57.66 | -5.60 | - | - |
| Quadratic* | 0.10 | 3.34 | 2.00 | 63.00 | 55.10 | 11.12 | -15.07 | - |
| Cubic** | 0.22 | 5.90 | 3.00 | 62.00 | 51.44 | 81.68 | -205.59 | 125.11 |
| Cu | | | | | | | | |
| Linear | 0.01 | 0.44 | 1.00 | 64.00 | 19.79 | -2.02 | - | - |
| Quadratic | 0.01 | 0.23 | 2.00 | 63.00 | 19.55 | -0.51 | -1.36 | - |
| Cubic | 0.08 | 1.83 | 3.00 | 62.00 | 16.43 | 59.76 | -164.11 | 106.87 |
| Mn | | | | | | | | |
| Linear* | 0.10 | 7.16 | 1.00 | 64.00 | 613.55 | -113.45 | - | - |
| Quadratic* | 0.15 | 5.38 | 2.00 | 63.00 | 562.51 | 219.23 | -299.70 | - |
| Cubic** | 0.26 | 7.19 | 3.00 | 62.00 | 506.11 | 1307.41 | -3238.31 | 1929.75 |
| Ni | | | | | | | | |
| Linear* | 0.09 | 6.64 | 1.00 | 64.00 | 29.14 | -4.28 | - | - |
| Quadratic* | 0.11 | 3.96 | 2.00 | 63.00 | 27.89 | 3.81 | -7.29 | - |
| Cubic** | 0.26 | 7.34 | 3.00 | 62.00 | 25.35 | 52.96 | -140.02 | 87.16 |
| V | | | | | | | | |
| Linear | 0.02 | 1.21 | 1.00 | 64.00 | 59.64 | -3.83 | - | - |
| Quadratic* | 0.10 | 3.29 | 2.00 | 63.00 | 54.43 | 30.09 | -30.56 | - |
| Cubic** | 0.19 | 4.93 | 3.00 | 62.00 | 50.29 | 110.12 | -246.67 | 141.92 |
| Zn | | | | | | | | |
| Linear | 0.00 | 0.25 | 1.00 | 64.00 | 64.98 | -3.08 | - | - |
| Quadratic | 0.02 | 0.51 | 2.00 | 63.00 | 61.36 | 20.50 | -21.24 | - |
| Cubic | 0.07 | 1.61 | 3.00 | 62.00 | 55.87 | 126.50 | -307.49 | 187.98 |

* $p < 0.05$.** $p < 0.01$.

Table 5
Comparison of models between different scales HII with metals.

| Scales | RSS | SS% | df | F | Ad-R ² |
|--------|-----------|-------|----|---------------------|-------------------|
| Cr | | | | | |
| C200 | – | – | – | – | – |
| C500 | 665.7 | 16.04 | 3 | 3.948 [*] | 0.12 |
| C1000 | 921.8 | 22.2 | 3 | 5.9 ^{**} | 0.18 |
| C1500 | 675.1 | 16.3 | 3 | 4.014 [*] | 0.12 |
| C2000 | 651 | 15.7 | 3 | 3.844 [*] | 0.12 |
| Mn | | | | | |
| C200 | 199,205.6 | 18 | 3 | 4.528 ^{**} | 0.14 |
| C500 | 144,975.8 | 13.08 | 3 | 9.631 ^{**} | 0.12 |
| C1000 | 286,186.7 | 25.8 | 3 | 7.194 ^{**} | 0.22 |
| C1500 | 213,768.0 | 19.3 | 3 | 4.939 ^{**} | 0.15 |
| C2000 | 258,287.8 | 23.3 | 3 | 6.28 ^{**} | 0.20 |
| Ni | | | | | |
| C200 | 230.5 | 13.66 | 3 | 3.268 [*] | 0.10 |
| C500 | 328.2 | 19.4 | 3 | 4.989 ^{**} | 0.16 |
| C1000 | 442.5 | 26.2 | 3 | 7.343 ^{**} | 0.23 |
| C1500 | 299.4 | 17.7 | 3 | 4.457 ^{**} | 0.14 |
| C2000 | 298.9 | 17.7 | 3 | 4.448 ^{**} | 0.14 |
| V | | | | | |
| C200 | – | – | – | – | – |
| C500 | 1026.7 | 13.1 | 3 | 3.632 [*] | 0.15 |
| C1000 | 1322.8 | 19.3 | 3 | 4.929 ^{**} | 0.15 |
| C1500 | – | – | – | – | – |
| C2000 | – | – | – | – | – |

* $p < 0.05$.

** $p < 0.01$.

disturbances indicators, which make our approach robust to understanding.

Hydrological processes play a key role in typical anthropogenic disturbances including agriculture, aquaculture, and solar salts production at the coastal region [51,52]. Within each scale circle plots, an easily posed question is how the anthropogenic disturbances induce the heavy metals. The study site is a coastal deposition plain, and the transportation rate at each soil sampling site is low [54]. So within each scope the heavy metals transported from other further region should be minimal. The hydrological processes play a key role in the metals transportation and deposition, but this process is human controlled within each soil sampling site.

The statistical models do not have an expected estimation result between the HII and heavy metals. It is not enough only using the landuse data to do spatial statistics [55–58]. The anthropogenic factors should include more detailed information in HII computing process. The potential research directions might include the detailed transportation and transformation research within the aquaculture water, the interaction between the offshore-sea water and the aquaculture landscape, the detailed substances and energy investment in agriculture and aquaculture in the HII computing process, and the geochemical cycling of the metals. But our study shows that the models between the heavy metals and HII have a meaningful result that the 1000 m scale's HII is the best model.

The present research is meaningful in these two aspects: (1) we give a quantitative approach to detect the spatial scale of the non-point source pollution, integrated the landuse data and the field soil survey data. In other regions, scientists can apply this analysis process to detect the spatial scale of human disturbances between HII calculated based on the local landuse patterns and concentrations of different hazardous materials and (2) the characteristic spatial scale of human disturbances is 1000 m, so we should analyse, characterize the human disturbances [1–5] and then make the responding policy in terms of HM controlled on this scale on the Yellow Sea coast. On the coast, the ecological conservation network [59] should have a buffer zone of 1000 m, not 200 m. Presently only the 200 m buffer zones from the wetland edge of the core region of the two national natural reserve lands are managed on the coast, and in the region beyond 200 m large amounts of lands have

been used to aquaculture, agriculture, or other human-dominated landuse.

6. Conclusion

We conclude that the characteristic spatial anthropogenic disturbances scale could be detected with our proposed methods, as defined by Findlay and Zheng [12]. From our analysis, the characteristic spatial anthropogenic disturbances scale along the Yellow Sea coast is 1000 m. Two new views should be updated into the coastal ecosystem management policy: (1) human disturbances should be managed with a larger scale of 1000 m and (2) a linked spatial ecological conservation network with buffer zones of 1000 m should be necessary to cope with the non-point source stressors.

Acknowledgements

Thanks Professor A.P. Cracknell for his valuable suggestions and revisions for the paper. Thanks a lot to the anonymous reviewers for their helpful comments on the manuscript. This work is partially supported by Natural Scientific Foundation of China (No. 40801068), Fund for Young Excellent Teachers by the Shanghai Education Committee (No. B-8101-09-0022), Starting Fund for Young Scientists by Shanghai Ocean University (No. B-8201-08-0280) and Shanghai Leading Academic Discipline Project (S30701).

References

- [1] S.A. Levin, The problem of pattern and scale in ecology, *Ecology* 73 (1992) 1943–1967.
- [2] J. Wu, O.L. Loucks, From balance-of-nature to hierarchical patch dynamics: a paradigm shift in ecology, *Q. Rev. Biol.* 70 (1995) 439–466.
- [3] G.D. Jenerette, J. Wu, On the definitions of scale, *Bull. Ecol. Soc. Am.* 81 (2000) 104–105.
- [4] J. Wu, Hierarchy and scaling: extrapolating information along a scaling ladder, *Can. J. Remote Sens.* 25 (1999) 367–380.
- [5] C.C. Gibson, E. Ostrom, T.K. Ahn, The concept of scale and the human dimensions of global change: a survey, *Ecol. Econ.* 32 (2000) 217–239.
- [6] J.L. Dungan, J.N. Perry, M.R.T. Dale, P. Legendre, M.J. Citron-Pousty, S. Fortin, A. Jakomulska, M.S. Miriti, M. Rosenberg, A balanced view of scale in spatial statistical analysis, *Ecography* 25 (2002) 626–640.

- [7] J. Wu, Y. Qi, Dealing with scale in landscape analysis: an overview, *Geogr. Inform. Sci.* 6 (2000) 1–5.
- [8] J. Wu, R. Hobbs, Key issues and research priorities in landscape ecology: an idiosyncratic synthesis, *Landscape Ecol.* 17 (2002) 355–365.
- [9] M. Rietkerk, K.L. Koppel, J.v.d. Langevelde, The ecology of scale, *Ecol. Modell.* 149 (2002) 1–4.
- [10] M.G. Turner, Landscape ecology: what is the state of the science? *Annu. Rev. Ecol. Syst.* 36 (2005) 319–344.
- [11] M.G. Turner, Landscape ecology in North America: past, present, and future, *Ecology* 86 (2005) 1967–1974.
- [12] C.S. Findlay, L. Zheng, Determining characteristic stressor scales for ecosystem monitoring and assessment, *J. Environ. Manage.* 50 (1997) 265–281.
- [13] K.N. Lee, *Compass and Gyroscope: Integrating Science and Politics for the Environment*, Island Press, Washington, DC, 1993.
- [14] J. Wu, Landscape ecology, cross-disciplinary, and sustainability science, *Landscape Ecol.* 21 (2006) 1–4.
- [15] R.E. Grumbine, What is ecosystem management? *Conserv. Biol.* 8 (1994) 27–38.
- [16] N.L. Christensen, A.M. Bartuska, J.H. Brown, S. Carpenter, C. D'Antonio, R. Francis, J.F. Franklin, J.A. Macmahon, R.F. Noss, D.J. Parsons, C.H. Peterson, M.G. Turner, R.G. Woodmansee, The report of the Ecological Society of American Committee on the scientific basis for ecosystem management, *Ecol. Appl.* 6 (1996) 665–691.
- [17] E. Joao, How scale affects environmental impact assessment, *Environ. Impact Assess. Rev.* 22 (2002) 289–310.
- [18] J.G. Liu, T. Dietz, S.R. Carpenter, M. Alberti, C. Folke, E. Moran, A.N. Pell, P. Deadman, T. Kratz, J. Lubchenco, E. Ostrom, Z.Y. Ouyang, W. Provencher, C.L. Redman, S.H. Schneider, W.W. Taylor, Complexity of coupled human and natural systems, *Science* 317 (2007) 1513–1516.
- [19] B.T. Werner, D.E. McNamara, Dynamics of coupled human-landscape systems, *Geomorphology* 91 (2007) 393–407.
- [20] G. Hodgson, A global assessment of human effects on coral reefs, *Mar. Pollut. Bull.* 38 (1999) 345–355.
- [21] H. Shi, A. Singh, Status and inter-connections of selected environmental issues in the global coastal zones, *Ambio* 32 (2003) 145–152.
- [22] N.G. Kragt, T.J. Zitman, M.J.F. Stive, Z.B. Wang, Morphological response of tidal basins to human interventions, *Coast. Eng.* 51 (2004) 207–221.
- [23] C. Small, R.J. Nicholls, A global analysis of human settlement in coastal zones, *J. Coast. Res.* 19 (2003) 584–599.
- [24] IGBP report 51 and IHDP report 18, Land–ocean interactions in the coastal zone (LOICZ) [online]. Available from: www.loicz.org, 2005 (cited 09.04.2006).
- [25] B.G.T.M. Peters, S.J.M.H. Hulscher, Large-scale offshore sand extraction: what could be the results of interaction between model and decision process? *Ocean. Coast. Manage.* 49 (2006) 164–187.
- [26] A. Baquirizo, M.A. Losada, Human interaction with large scale coastal morphological evolution. An assessment of the uncertainty, *Coast. Eng.* 55 (2008) 569–580.
- [27] R.G. Martone, K. Wasson, Impacts and interactions of multiple human perturbations in a California salt marsh, *Oecologia* 158 (2008) 151–163.
- [28] C.S. Findlay, J. Bourdages, Response time of wetland biodiversity to road construction on adjacent lands, *Conserv. Biol.* 14 (1999) 86–94.
- [29] J.E. Houlahan, The effects of adjacent land-use on water quality and biodiversity in southeastern Ontario wetlands, Doctoral Thesis, University of Ottawa, 2002.
- [30] R.B. Owen, N. Sandhu, Heavy metal accumulation and anthropogenic impacts on Tolo Harbour, Hong Kong, *Mar. Pollut. Bull.* 40 (2000) 174–180.
- [31] Q.S. Kang, J.Z. Zhou, Y. Wu, J. Zhang, Distribution and research situation of heavy metals in tidal wetlands of Changjiang Estuary, *Mar. Environ. Sci.* 22 (2003) 44–47 (in Chinese with English abstracts).
- [32] L. Qiao, X.Y. Yuan, A.M. Li, Heavy metals in littoral zone of Jiangsu Province and an ecological risk evaluation of heavy metals to this zone, *J. Agro-Environ. Sci.* 24 (2005) 178–182 (in Chinese with English abstracts).
- [33] L.Y. Liu, G.M. Sun, P.Y. Liu, J.H. Tang, M.R. Zhang, An analysis on the inshore water quality on the Lusi fishing grounds by principal component analysis (PCA) and cluster analysis, *Mar. Fish.* 28 (2006) 217–221 (in Chinese with English abstracts).
- [34] Q.S. Li, B. Chu, L. Shi, J.H. Fang, S.S. Chai, Heavy metal distribution in tidal wetland soils and its effect on reclamation in the Pearl River Estuary, *J. Agro-Environ. Sci.* 26 (2007) 1422–1426 (in Chinese with English abstracts).
- [35] X.H. Wang, X.Q. Zou, W.J. Yu, Heavy metal contamination in coastal sediments of Wanggang, Jiangsu Province, *J. Agro-Environ. Sci.* 26 (2007) 784–789 (in Chinese with English abstracts).
- [36] W.J. Yu, X.Q. Zou, The accumulation law and pollution estimation of heavy metals of Pb, Cu, and Zn from Wanggang tidal flat, *Geogr. Res.* 26 (2007) 809–820 (in Chinese with English abstracts).
- [37] B. Deng, J. Zhang, G.R. Zhang, J.Z. Zhou, Enhanced anthropogenic heavy metal dispersal from tidal disturbance in the Jiaozhou Bay, North China, *Environ. Monit. Assess.* (2009), doi:10.1007/s10661-009-0751-x.
- [38] J.L. Li, M. He, W. Han, Y.F. Gu, Analysis and assessment on heavy metal sources in the coastal soils developed from alluvial deposits using multivariate statistical methods, *J. Hazard. Mater.* 164 (2009) 976–981.
- [39] R.P. Brooks, Monitoring and assessment data use and application: establishing common measurement endpoints for ambient assessments, Juata case study, National Biological Assessment and Criteria Workshop, WET101-11, 2003.
- [40] R.P. Brooks, D.H. Wardrop, J.A. Bishop, Assessing wetland condition on a watershed basis in the mid-Atlantic region using synoptic land-cover maps, *Environ. Monit. Assess.* 94 (2004) 9–22.
- [41] M.T. Brown, M.B. Vivas, A landscape development intensity index, *Environ. Monit. Assess.* 101 (2005) 289–309.
- [42] S.B. Fang, X.S. Zhang, X.B. Jia, S.Q. An, C.F. Zhou, C. Xu, Evaluation of potential habitat with an integrated analysis of a spatial conservation strategy for David's Deer, ELAPHURUS DAVIDIANS, *Environ. Monit. Assess.* 150 (2009) 455–468.
- [43] J.D. Wickham, R.V. O'Neil, K.B. Jones, A geography of ecosystem vulnerability, *Landscape Ecol.* 15 (2000) 495–504.
- [44] IUSS Working Group WRB, World Reference Base for Soil Resources 2006. World Soil Resources Reports No. 103, FAO, Rome, 2006.
- [45] R.H.C. Emmerson, S.B. O'Reilly-Wiese, C.L. Macleod, J.N. Lester, A multivariate assessment of metal distribution in inter-tidal sediments of the Blackwater Estuary, UK, *Mar. Pollut. Bull.* 34 (1997) 960–968.
- [46] A.E. Nemr, A. Khaled, A.E. Sikaily, Distribution and statistical analysis of leachable and total heavy metals in the sediments of the Suez Gulf, *Environ. Monit. Assess.* 118 (2006) 89–112.
- [47] K. McGarigal, B.J. Marks, FRAGSTATS: spatial pattern analysis program for quantifying landscape structure, US Department of Agriculture, Forest Service, Pacific Northwest Research Station, Portland, OR. General Technical Report, PNW-GTR-351, 1995, p. 120.
- [48] K.H. Riitters, R.V. O'Neill, C.T. Hunsaker, J.D. Wichham, D.H. Yankee, K.B.J. Timmins, B.L. Jackson, A factor analysis of landscape pattern and structure metrics, *Landscape Ecol.* 10 (1995) 23–39.
- [49] J.P. Wang, Study on coastal environmental evaluation and early warning system, Yancheng, Jiangsu Province, Doctoral Thesis, Nanjing University, 2006 (in Chinese with English abstract).
- [50] C.S. Findlay, J. Houlahan, Anthropogenic correlates of species richness in south-eastern Ontario wetlands, *Conserv. Biol.* 11 (1997) 1000–1009.
- [51] P. Visuthismajarn, B. Vitayavirasuk, N. Leeraphante, M. Kietpawpan, Ecological risks assessment of abandoned shrimp ponds in southern Thailand, *Environ. Monit. Assess.* 104 (2005) 409–418.
- [52] S. Caeiro, M.H. Costa, T.B. Ramos, F. Fernandes, N. Silveira, A. Coimbra, G. Medeiros, M. Painho, Assessing heavy metal contamination in Sado Estuary sediment: an index analysis approach, *Ecol. Indic.* 5 (2005) 151–169.
- [53] O. Firat, G. Gok, H.Y. Cogun, T.A. Yuzereroglu, F. Kargin, Concentrations of Cr, Cd, Cu, Zn and Fe in crab *Charybdis longicollis* and shrimp *Penaeus semisulcatus* from the Iskenderum Bay, Turkey, *Environ. Monit. Assess.* 147 (2008) 117–123.
- [54] M.E. Ren, Beach lands exploitation in China: present situations and counter-measures, *J. CAS (Special Issue)* (1996) 440–443 (in Chinese).
- [55] L. Fahrig, J.H. Pedlar, S.E. Pope, P.D. Taylor, J.F. Wegner, Effect of road traffic on amphibian density, *Biol. Conserv.* 73 (1995) 177–182.
- [56] K.A. With, D.M. Pavuk, J.L. Worchuck, R.K. Oates, J.L. Fisher, Threshold effects of landscape structure on biological control in agroecosystems, *Ecol. Appl.* 12 (2002) 52–65.
- [57] N. Blaum, E. Rossmanith, F. Jeltsch, Land use affects rodent communities in Kalahari savannah rangelands, *Afr. J. Ecol.* 45 (2007) 189–195.
- [58] N. Lemoine, H.G. Bauer, M. Peintinger, K.B. Gaese, Effects of climate and land-use change on species abundance in a central European Bird Community, *Conserv. Biol.* 21 (2007) 495–503.
- [59] T.S. Hocht, M.H. Carr, P.D. Zwick, Identifying a linked reserve system using a regional landscape approach: the Florida ecological network, *Conserv. Biol.* 14 (2000) 984–1000.